Engineering -oxidation in Yarrowia lipolytica for methyl ketone production

Hanko, Erik K. R.; Denby, Charles M.; Nogué, Violeta Sànchez I; Lin, Weiyin; Ramirez, Kelsey J.; Singer, Christine A.; Beckham, Gregg T.; Keasling, Jay D.

Published in:
Metabolic Engineering

Link to article, DOI:
10.1016/j.ymben.2018.05.018

Publication date:
2018

Document Version
Peer reviewed version

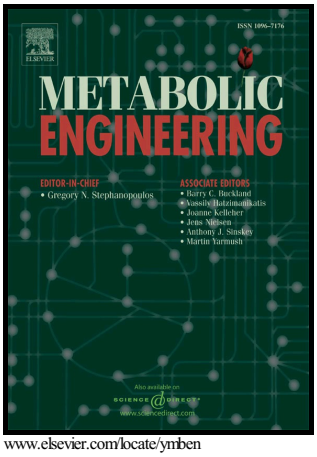

www.elsevier.com/locate/ymben

Engineering β-oxidation in *Yarrowia lipolytica* for methyl ketone production

Erik K.R. Hanko, Charles M. Denby, Violeta Sànchez i Nogué, Weiyin Lin, Kelsey J. Ramirez, Christine A. Singer, Gregg T. Beckham, Jay D. Keasling

PII: S1096-7176(17)30463-9
DOI: https://doi.org/10.1016/j.ymben.2018.05.018
Reference: YMBEN1416

To appear in: *Metabolic Engineering*

Received date: 12 December 2017
Revised date: 14 May 2018
Accepted date: 27 May 2018

Cite this article as: Erik K.R. Hanko, Charles M. Denby, Violeta Sànchez i Nogué, Weiyin Lin, Kelsey J. Ramirez, Christine A. Singer, Gregg T. Beckham and Jay D. Keasling, Engineering β-oxidation in *Yarrowia lipolytica* for methyl ketone production, *Metabolic Engineering*, https://doi.org/10.1016/j.ymben.2018.05.018

Engineering β-oxidation in *Yarrowia lipolytica* for methyl ketone production

Erik K. R. Hanko[a,b,12,], Charles M. Denby[a,b,c,2], Violeta Sànchez i Nogué[d], Weiyin Lin[a], Kelsey J. Ramirez[e], Christine A. Singer[d], Gregg T. Beckham[d], Jay D. Keasling[a,b,f,g,h,i*]

[a]DOE Joint BioEnergy Institute, 5885 Hollis St., Emeryville, CA 94608, United States

[b]Biological Systems and Engineering Division, Lawrence Berkeley National Laboratory, Berkeley, CA 94720, United States

[c]California Institute of Quantitative Biosciences (QB3), University of California, Berkeley, CA 94720, United States

[d]National Bioenergy Center, National Renewable Energy Laboratory, Golden, CO 80401, United States

[e]Biosciences Center, National Renewable Energy Laboratory, Golden, CO 80401, United States

[f]Department of Chemical and Biomolecular Engineering, University of California, Berkeley, CA 94720, United States

[g]Department of Bioengineering, University of California, Berkeley, CA 94720, United States

[h]The Novo Nordisk Foundation Center for Biosustainability, Technical University of Denmark, Building 220, Kemitorvet, 2800 Kgs, Lyngby, Denmark

[i]Center for Synthetic Biochemistry, Institute for Synthetic Biology, Shenzhen Institutes for Advanced Technologies, Shenzhen, China

[1] Present address: BBSRC/EPSRC Synthetic Biology Research Centre (SBRC), The University of Nottingham, Nottingham, NG7 2RD, United Kingdom

[2] These authors contributed equally to this work as the first authors.

*Corresponding author at: DOE Joint Bioenergy Institute, 5885 Hollis St., Emeryville, CA 94608, Unites States. *E-mail address:* jdkeasling@lbl.gov (J.D. Keasling).

Abstract

Medium- and long-chain methyl ketones are fatty acid-derived compounds that can be used as biofuel blending agents, flavors and fragrances. However, their large-scale production from sustainable feedstocks is currently limited due to the lack of robust microbial biocatalysts. The oleaginous yeast *Yarrowia lipolytica* is a promising biorefinery platform strain for the production of methyl ketones from renewable lignocellulosic biomass due to its natively high flux towards fatty acid biosynthesis. In this study, we report the metabolic engineering of *Y. lipolytica* to produce long- and very long-chain methyl ketones. Truncation of peroxisomal β-oxidation by chromosomal deletion of *pot1* resulted in the biosynthesis of saturated, mono-, and diunsaturated methyl ketones in the C_{13}-C_{23} range. Additional overexpression and peroxisomal targeting of a heterologous bacterial methyl ketone biosynthesis pathway yielded an initial titer of 151.5 mg/L of saturated methyl ketones. Dissolved oxygen concentrations in the cultures were found to substantially impact cell morphology and methyl ketone biosynthesis. Bioreactor cultivation under optimized conditions resulted in a titer of 314.8 mg/L of total methyl ketones, representing more than a 6,000-fold increase over the parental strain. This work highlights the potential of *Y. lipolytica* to serve as chassis organism for the biosynthesis of acyl-thioester derived long- and very long-chain methyl ketones.

Keywords

Methyl ketones, *Yarrowia lipolytica*, Metabolic engineering, Beta-oxidation, Peroxisome, Fatty acid metabolism

1. Introduction

In recent years, fatty acid-derived biofuels have gained increasing interest as an alternative to petroleum-based fuels (Li et al., 2008; Xu et al., 2016). Every mole of carbon that is emitted when burning as a fuel was originally captured from the atmosphere by the biofuel crop, whereas combustion of petroleum-derived fuel results in a net gain of atmospheric carbon contributing to global warming. The most common commercially available fatty acid-derived biofuel today is biodiesel, which is composed of fatty acid alkyl esters. When combusted, less greenhouse gases and air pollutants such as particulate matter, carbon monoxide, or sulfur oxides are emitted compared to petroleum-derived diesel (Hill et al., 2006; Liu et al., 2012; Sheehan et al., 1998). The physical properties of fatty acid-derived biofuels are similar to petroleum-based diesel, which makes biodiesel compatible with existing storage and transportation infrastructure (Peralta-Yahya and Keasling, 2010). However, the main drawback of biodiesel is that mainly food-based crops are employed as raw material for its production. To overcome the dependency on petroleum supplies and to reduce impact on food prices, substantial research efforts have been directed towards developing microbial platforms, such as oleaginous yeasts, for overproduction of fatty acids from non-edible lignocellulosic feedstocks (Angerbauer et al., 2008; Chi et al., 2011; Galafassi et al., 2012), which can ultimately be turned into sustainable biofuel by chemical- or microbial processes (Pfleger et al., 2015). Apart from fatty acid alkyl esters, several acyl thioester-derived compounds including fatty alcohols, methyl ketones, or dicarboxylic acids were reported to have desirable fuel properties (Clomburg et al., 2015; d'Espaux et al., 2015; Feng et al., 2015; Goh et al., 2012).

One of the most extensively studied non-conventional yeasts is *Yarrowia lipolytica*. It is considered an oleaginous microorganism due to its ability to accumulate lipids at levels of more than 20% of its biomass (Ratledge and Wynn, 2002). As it name implies, *Y. lipolytica* is capable of growing on hydrophobic substrates as sole source of carbon by secreting extracellular lipases and can often be found in lipid-rich environments such as dairy products or oil (Barth and Gaillardin, 1997; Fickers et al., 2005; Pignède et al., 2000). A main focus of *Y. lipolytica* research to date has been the

elucidation of the mechanisms of fatty acid biosynthesis, hydrophobic substrate utilization, and lipid degradation, also referred to as β-oxidation.

In *Y. lipolytica*, medium- and long-chain acyl-CoAs are degraded in peroxisomes to produce energy through β-oxidation (Fig. 1). Both acyl-CoAs formed in the cytoplasm and fatty acids are transported across the peroxisomal membrane (Dulermo et al., 2015). The first reaction of the native *Y. lipolytica* β-oxidation pathway is catalyzed by an acyl-CoA oxidase complex (Titorenko et al., 2002). Six genes, *POX1* to *POX6*, are involved in FAD-dependent oxidation of acyl-CoA to *trans*-2,3-dehydroacyl-CoA. Both the hydration to β-hydroxyacyl-CoA and the subsequent dehydrogenation to β-ketoacyl-CoA are catalyzed by the multifunctional enzyme MFE. The thiolytic cleavage of β-ketoacyl-CoA results in an acetyl-CoA and an acyl-CoA with two fewer carbons, completing one cycle of β-oxidation. This final step is catalyzed by the acetyl-CoA acyltransferase POT1 (Beopoulos et al., 2009). Our understanding of these processes in *Yarrowia* was greatly facilitated by similar mechanisms in the well-characterized model organism *S. cerevisiae*. However, *Y. lipolytica* natively has higher flux towards lipid synthesis and storage within lipid bodies and therefore may serve as a more suitable chassis for production of lipid-derived biofuels (Beopoulos et al., 2009). This oleaginous yeast has been engineered so far to produce fatty acid methyl esters at titers of approximately 99 g/L (Qiao et al., 2017). Furthermore, it has been employed for the production of γ-lactone and hexanal, which find broad application in the flavor and fragrance industry (Bourel et al., 2004; Schrader et al., 2004), as well as the food supplements β-carotene and omega-3 and omega-6 fatty acids (Gao et al., 2017; Xue et al., 2013).

Aliphatic methyl ketones, another group of fatty acid-derived compounds, are commonly found as constituents of essential oils of various plant species (Thoms, 1903; Walbaum and Hüthig, 1902; Williams, 1858) and used as volatile and non-volatile pheromones by mammals or reptiles (Mason et al., 1989). Medium-chain methyl ketones are employed in the flavor and fragrance industry, and have desirable properties for use as diesel fuel blending agents (Goh et al., 2012; Longo and Sanromán, 2006). They have the potential to be better biofuel product targets than other fatty

acid-derived compounds such as fatty alcohols, which require additional downstream processing steps to be extracted. Methyl ketones, on the other hand, permeate the plasma membrane via passive diffusion and can be captured by overlaying the culture with an organic solvent. The highest titer reported so far was achieved by fed-batch glucose fermentation (2.2% w/v) of engineered *E. coli* DH1 resulting in 3.4 g/L of C_{11} to C_{15} methyl ketones (Goh et al., 2014). This engineered strain comprised the following features: (i) overproduction of β-ketoacyl-CoAs through a re-engineered β-oxidation pathway, (ii) overexpression of the native thioesterase FadM, and (iii) balanced overexpression of the fatty acyl-CoA synthetase, FadD, and the fatty acid-responsive transcription factor FadR (Goh et al., 2014). Another approach to obtain methyl ketones in *E. coli* MG1655 was pursued by Park and co-workers (Park et al., 2012). Their engineering strategy was based on overexpressing a 3-ketoacyl-acyl carrier protein (ACP) thioesterase and a β-decarboxylase from the wild tomato *Solanum habrochaites*. Under optimal levels of oxygen, glucose batch incubation (5% w/v) of the best performing strain led to a methyl ketone titer of approximately 500 mg/L (Park et al., 2012). Moreover, the methyl ketone biosynthesis pathway developed by Goh and co-workers was transferred to the facultative chemolithoautotrophic bacterium *Ralstonia eutropha* H16 (Müller et al., 2013). Under autotrophic growth conditions with CO_2 and H_2 as sole source of carbon and energy, it was able to accumulate diesel-range methyl ketones up to 180 mg/L (Müller et al., 2013). Due to its physiology, *Y. lipolytica* may be a more robust chassis for an industrial-scale production of diesel-range methyl ketones. Further advantages include (i) a well-studied fatty acid metabolism, (ii) a natively high flux towards lipid biosynthesis, (iii) the availability of a broad range of genetic tools that allow metabolic engineering for the production of acyl thioester-based compounds, and (iv), its ability to grow on biomass hydrolysates derived from sustainable lignocellulosic feedstocks (Chi et al., 2011; Patel et al., 2016; Yu et al., 2011).

In this study, we engineered the oleaginous yeast *Y. lipolytica* to produce diesel-range methyl ketones for use as biofuel blending agents and as flavors and fragrances. Batch fermentation of the

best strain, which comprised a truncated β-oxidation pathway and an integrated heterologous bacterial methyl ketone biosynthesis pathway, resulted in a final methyl ketone titer of 314.8 mg/L.

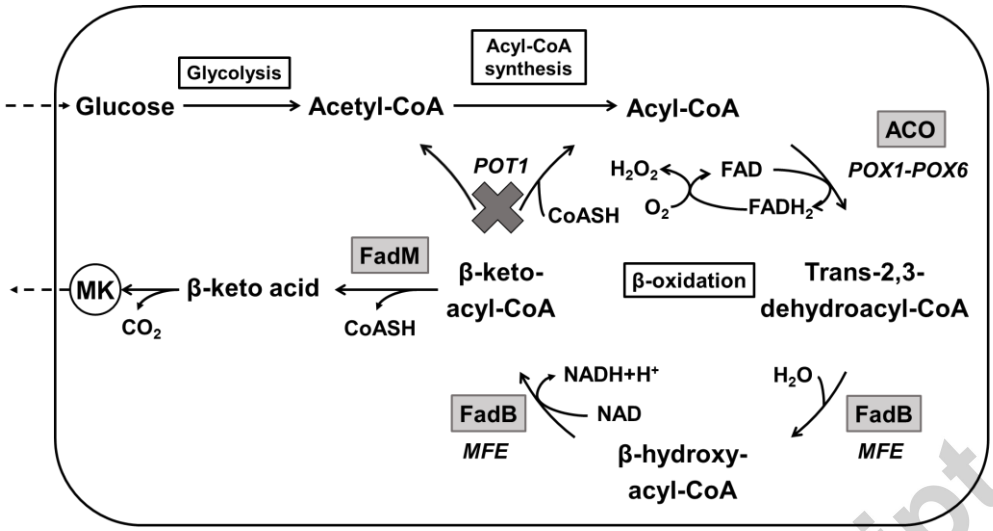

Fig. 1. The engineered β-oxidation pathway in *Y. lipolytica* for production of methyl ketones. Native enzymes involved in β-oxidation are italicized. Heterologously expressed enzymes of the bacterial methyl ketone biosynthesis pathway are highlighted in grey boxes. The chromosomal deletion of the gene encoding the acetyl-CoA acyltransferase, POT1, is illustrated as a cross. The ultimate methyl ketone (MK) product is highlighted as a circle.

2. Materials and methods

2.1. Base strains and media

Escherichia coli HST08 (Clontech Laboratories, Inc.) was used for cloning and plasmid propagation. *E. coli* was grown at 37°C in LB medium (EMD Millipore) supplemented with the appropriate antibiotic at the following final concentration: 100 µg/mL of carbenicillin, 25 µg/mL of chloramphenicol, and 50 µg/mL of kanamycin. The *Y. lipolytica* derivatives were engineered from the base strain PO1f (ATCC MYA-2613) and were cultivated at 30°C unless indicated otherwise (Madzak et al., 2000). When necessary, hygromycin B was added to a concentration of 200 µg/mL.

YPD medium consisted of 10 g/L yeast extract (Becton, Dickinson and Company), 20 g/L peptone (Becton, Dickinson and Company), and 20 g/L glucose. YSC medium was prepared from 6.7 g/L Yeast Nitrogen Base w/o amino acids (Becton, Dickinson and Company), 2.37 g/L CSM (Sunrise Science Products), and 20 g/L glucose. To prepare YSC-LEU or YSC-URA medium, CSM was replaced by 2.07 g/L CSM-LEU or 2.31 g/L CSM-URA (Sunrise Science Products), respectively. For solid media, 15 g/L agar was added.

2.2. Cloning and transformation

E. coli plasmid DNA minipreps were performed using the QIAGEN QIAprep Spin Miniprep Kit. *Y. lipolytica* genomic DNA was extracted employing the Promega Wizard Genomic DNA Purification Kit. For cloning, DNA was amplified by PCR using the Phusion™ Hot Start II High-Fidelity Polymerase (Thermo Fisher Scientific) in 50 µL reactions under the recommended conditions. Restriction enzymes were purchased from New England Biolabs or Thermo Fisher Scientific, and digestions were set up according to the manufacturer's protocol. The Zymoclean™ Gel DNA Recovery Kit was employed to extract gel-purified linearized DNA, which was subsequently used for transformation or cloning.

Transformation of *E. coli* HST08 was performed using heat shock as recommended by the manufacturer. Transformation of *Y. lipolytica* with episomal overexpression plasmids or linearized

integration cassettes was done as described previously (Chen et al., 1997). Briefly, the strain that was to be transformed was spread on YPD agar and incubated at 30°C for 18 hours. Cells from the plate were resuspended in liquid YPD. 0.75 OD_{600} × mL cells were transferred to a microfuge tube and centrifuged at 2,000 × *g* for 30 s. The cells were resuspended in 100 µL one-step buffer and transferred to another tube that contained the DNA. One-step buffer was freshly prepared and consisted of 45% (w/v) PEG 3350, 100 mM dithiothreitol, 100 mM lithium acetate (pH 6.0), and 250 µg/mL salmon sperm single-stranded carrier DNA. Usually, 100 ng of uncut plasmid DNA or 300 ng of linearized DNA were transformed. The transformation mix was vortexed and incubated at 39°C for 1 hour. The entire mixture was subsequently spread on the appropriate well-dried pre-warmed selective plate and incubated at 30°C for 36-48 hours.

2.3. Plasmid construction

Oligonucleotide primers were designed using the DNA assembly automation software j5 (Hillson et al., 2011) and synthesized by Integrated DNA Technologies. Primer sequences are listed in Table S1. *E. coli fadM* (*Ec*DH1_3166) was codon-optimized using the *Y. lipolytica* codon usage and the *E. coli fadB* (*Ec*DH1_4135), and the *Micrococcus luteus aco* (*Mlut*_11700) were codon-optimized for *S. cerevisiae* codon usage. The genes were synthesized by Integrated DNA Technologies. For Golden Gate Assembly, BsaI, BsmBI, and NotI restriction sites were manually removed by nucleotide exchange. Plasmids were assembled either by Gibson or Golden Gate (Gibson et al., 2009; Lee et al., 2015).

The Gibson Assembly Master Mix (New England Biolabs) was used for Gibson assembly and employed according to the manufacturer's protocol. The Golden Gate toolkit (AddGene), that was developed for DNA assembly in *S. cerevisiae* (Lee et al., 2015), was employed for Golden Gate assembly. For the toolkit to be also applied in *Y. lipolytica*, part plasmids were constructed that contain *Y. lipolytica* promoters, terminators, a selection marker, and homologous regions that allow for chromosomal integration. The structure of each element and the Golden Gate Assembly protocol were described previously (Lee et al., 2015). *Y. lipolytica* promoters and terminators that were

employed for assembly of gene constructs are listed in Table S2. All antibiotic or auxotrophic selection markers that were utilized to screen for successful integration into the *Y. lipolytica* genome were flanked with *loxP* sites to enable marker retrieval (Fickers et al., 2003). Cloned coding sequences and Golden Gate part plasmids were verified by DNA sequencing, which was performed by Quintara Biosciences (Berkeley, CA). A detailed assembly description for each plasmid is given in the Supplementary Materials. Key features of all plasmids used and generated in this study are summarized in Table S3. Maps of plasmids constructed in this study are available from the public version of the JBEI Registry (https://public-registry.jbei.org: entries JPUB_009513 to JPUB_009536).

2.4. Strain construction

Chromosomal deletions of *pot1* and *TEc1* were performed by transforming deletion cassettes into *Y. lipolytica*, which allow for homologous recombination. They consist of the *ura3* gene from *Kluyveromyces lactis* driven by the *Y. lipolytica exp1* promoter and flanked by *loxP* sites to enable marker retrieval (Damude et al., 2011; Fickers et al., 2003). This inner part of the cassette in turn is flanked by at least 1 Kb upstream and downstream homologous regions of the gene to be deleted. For deletion of *pot1* or *TEc1*, plasmids pEHYl018 or pEHYl090 were employed, respectively. Prior to transformation, plasmids were linearized by restriction digest with AlwNI and gel-purified.

Integration of overexpression cassettes was also performed by homologous recombination. The *E. coli fadM*-SKL integrative plasmid, pEHYl062, was constructed by Gibson cloning (Gibson et al., 2009) the UAS1B$_1$-TEF-*fadM*-SKL-cyc1t cassette from pEHYl051 between the *loxP* site upstream of *ura3* and the *E. coli* origin of replication of plasmid pEHYl018. The *fadB*-SKL and *aco*-SKL integrative plasmid, pEHYl087, was assembled by Golden Gate reaction of plasmids pEHYl074, pEHYl085, and pEHYl086. Prior to transformation, the plasmids pEHYl062 or pEHYl087 were linearized by restriction digest with ScaI or NotI, respectively, and gel-purified.

Successful integration of deletion and overexpression cassettes was confirmed by colony PCR using the oligonucleotide primers listed in Table S4. Colony PCR was performed using the GoTaq® Green Master Mix (Promega) according to the manufacturer's instructions.

Markerless strains were obtained as described previously by transformation and subsequent removal of plasmid pMCS-UAS1B$_{16}$-TEF-Cre (Blazeck et al., 2014; Fickers et al., 2003). This plasmid constitutively expresses a recombinase that recognizes the *loxP* sites flanking a selection marker to excise the marker gene. Successful marker retrieval and plasmid removal was confirmed by replica plating the strain on the appropriate dropout plate.

Expression of heterologous enzymes was confirmed by protein extraction, quantification, digestion, and electrospray ionization liquid chromatography-tandem mass spectrometry as described previously (Batth et al., 2012). All strains used and constructed in this study are listed in Table 1.

2.5. Microbial growth

E. coli and *Y. lipolytica* were grown in 60-mL culture tubes at 200 rpm unless indicated otherwise. For analysis of heterologous gene expression in *Y. lipolytica*, 10 mL of YPD were directly inoculated from glycerol stocks and grown for 24 hours before the cells were centrifuged for protein preparation.

For methyl ketone production in cells containing episomal expression cassettes, 5 mL of YSC without the appropriate amino acid were directly inoculated with a single colony from the freshly transformed yeast cells and cultivated for 18 hours. Ten mL of the same medium was inoculated with the previously-described culture to an OD_{600} of 0.05. Eighteen hours after inoculation, 1 mL of dodecane amended with 0.1 mg/mL of 3-tetradecanone (as an internal standard) was added to the culture. The cells were cultivated for another 48 hours before the dodecane overlay was sampled for direct gas chromatography-mass spectrometry (GC/MS) analysis.

The same protocol was employed for strains that were analyzed for the effect of chromosomal deletions and integrative expression cassettes on methyl ketone production with the following modifications: yeast cells were streaked onto a YPD plate from the glycerol stock and grown for 24 hours. To ensure optimal viability of cells, a single colony was taken, spread onto a fresh YPD plate, and grown for another 24 hours. The preculture was inoculated with a single colony from this plate.

The influence of dissolved oxygen concentration on methyl ketone production in EHYL01 (Δ*pot1*) was tested in baffled and non-baffled shake flasks. Five mL of YPD were directly inoculated from a glycerol stock and grown for 24 hours in culture tubes. Fifty mL of fresh YPD in 250 mL shake flasks was inoculated with the previously-described culture to an OD_{600} of 0.05. After 24 hours (200 rpm), cells were harvested and stained with Nile red for fluorescence microscopy.

2.6. Gas chromatography-mass spectrometry (GC/MS) analysis

Methyl ketones were analyzed by GC/MS. Samples (0.2 mL) of the dodecane overlay were removed from each culture and clarified by centrifugation at 15,000 × *g* and room temperature for 1 min. When necessary, the dodecane overlay was diluted with ethyl acetate. Culture tube samples were analyzed using an Agilent 6890 series GC equipped with a DB-5ms column (30 m length, 250 µm diameter, 0.25 µm film thickness, J & W 122-5532G) coupled to an Agilent 5973 mass selective detector (MSD). Samples and standards from the bioreactor cultivations were analyzed by an Agilent 7890A GC equipped with a CP-Sil 8 CB capillary column (30 m length, 250 µm diameter, 0.25 µm film thickness, Agilent J & W Scientific) coupled to an Agilent 5975C MSD with a triple axis detector. Samples of 1 µL were injected by an autosampler. The GC oven program was as follows: 40°C for 3 min, a ramp of 15°C/min to 240°C and a hold for 3 min, a ramp of 20°C/min to 300°C and a hold for 2 min. Carrier gas of high-purity helium was kept at a constant flow rate of 0.8 mL/min. The MS was operated in SCAN mode and molecular ions were typically scanned from 35 to 575 atomic mass units. Authentic standards of 2-tridecanone (Sigma-Aldrich), 2-pentadecanone (Sigma-Aldrich), 2-heptadecanone (Sigma-Aldrich), and 2-nonadecanone (Santa Cruz Biotechnology) were used for external standard quantification of saturated methyl ketones (*m/z* 58) from culture tube samples. Samples and standards from the bioreactor cultivations were spiked with *o*-terphenyl (AccuStandard) as internal standard to a final concentration of 0.04 g/L, to allow for internal quantification, and adjusted for any detector response shift. Since no authentic standards were available for unsaturated methyl ketones, they were quantified by employing the total ion chromatogram and the standards of the saturated species with the same carbon chain length. The Agilent MSD ChemStation software

was employed for data analysis. The reported methyl ketone titers refer back to the aqueous phase (C_{aq}) at a given time (i) using a V/V correction factor of $C_{aq,i} = C_{org,i} \times (V_{org,i} / V_{aq,i})$.

2.7. Nile red staining and microscopy

Nile red, 9-diethylamino-5H-benzo-α-phenoxazine-5-one, was employed for the visualization of cell morphology by fluorescence microscopy (Greenspan et al., 1985). Nile red staining was performed as described previously (Blazeck et al., 2014). One OD_{600} × mL cultures were harvested by centrifugation for 3 min at 1,000 × *g*. The supernatant was removed and cells were resuspended in 500 µL phosphate-buffered saline solution. To the cells, 6 µL of 1 mM Nile red was added. The Nile red was evenly distributed by flipping the tube and the cells were incubated for 15 min at room temperature in the dark. After incubation, the stained cells were centrifuged for 3 min at 1,000 × *g* and washed twice with ice cold water prior to fluorescence microscopic analysis. Micrographs were acquired on a Zeiss LSM 710 scanning confocal microscope with an oil immersion lens (100 × magnification, 1.4 numerical aperture) using ZEN 2009 software (Zeiss).

2.8. Bioreactor cultivations

The wild type strain PO1f and the optimal producing strain EHYL12 were analyzed for methyl ketone biosynthesis in bioreactors. Strains were streaked from glycerol stocks onto YPD agar plates and incubated at 28°C for 38 hours. Fifteen-mL glass tubes containing five mL of YPD were inoculated with a single colony, and cells were cultivated in a roller drum (New Brunswick Scientific TC-7, Eppendorf) at 28°C for 15 hours. Seed cultures were subsequently used to inoculate 0.5-L BIOSTAT® Qplus bioreactors (Sartorius) containing 300 mL of YPD to an initial OD_{600} of 0.1. The temperature was maintained at 28°C, and the pH was maintained at 5.2 by addition of 1 M KOH. Agitation was maintained constant at 100 rpm, and the dissolved oxygen level was set at 5% by adjusting the air supply (from 0.3 mL/min to 1 mL/min). When the OD_{600} of the cultivation exceeded 1.0, 60 mL dodecane, amended with 0.1 mg/mL 3-tetradecanone as a surrogate, was added to the bioreactor. Upon sugar depletion after around 101 hours, 33 mL of 200 g/L sterile glucose were pulsed into the bioreactors with cultures of strain EHYL12. Samples for OD_{600} measurements and metabolite analysis

in the cultivation medium and the dodecane overlay were taken regularly until sugar depletion. Cells in the cultivation broth were separated by centrifugation; the supernatant was filtered through a 0.2 µm membrane filter and stored at -20°C until analysis.

2.9. Metabolite analysis from bioreactor cultivations

Glucose, pyruvate, acetate, succinate, glycerol, ethanol and mannitol concentrations were determined by high-performance liquid chromatography (HPLC). The analysis was performed using an Agilent 1100 LC system equipped with an Aminex HPX-87H 300 mm × 7.8 mm × 9 µm column (BioRad), a G1362A refractive index detector and a G1365B multiple wavelength detector (Agilent Technologies). The column was operated at 55°C with an isocratic flow rate of 0.6 mL/min 0.01 M H_2SO_4 and a sample injection volume of 20 µL. Glucose, acetate, succinate, glycerol, ethanol, and mannitol were quantified using the refractive index detector and pyruvate using the multiple wavelength detector set at 210 nm.

3. Results

3.1. Truncation of peroxisomal β-oxidation results in accumulation of methyl ketones

For more than ninety years, fungi have been known to produce methyl ketones (Stärkle, 1924). The pathway by which they are formed has been elucidated as an abortive β-oxidation of fatty acids followed by a decarboxylation of β-keto acids (Forney and Markovetz, 1971) (Fig. 1). In *E. coli*, the native thioesterase FadM converts β-ketoacyl-CoAs to β-keto acids (Goh et al., 2012). The subsequent decarboxylation of β-keto acids to methyl ketones occurs spontaneously (Goh et al., 2014). In yeast, no thioesterases have been reported that catalyze this reaction. However, the fact that small amounts of 2-heptadecanone (C17:0 methyl ketone) were detected in the *Y. lipolytica* base strain PO1f led to the hypothesis that a yet unknown native thioesterase may convert β-ketoacyl-CoAs to β-keto acids.

To test this hypothesis, the gene encoding the peroxisomal acetyl-CoA acyltransferase, *pot1* (YALI0E18568g), was deleted by homologous recombination. We anticipated that deletion of *pot1* would remove the thiolytic cleavage activity required for the terminal step of β-oxidation, resulting in the hydrolysis of β-ketoacyl-CoAs by an as of yet unknown native thioesterase.

The strains were initially grown in aqueous rich media. After cultures achieved a high density, a dodecane overlay was added to partition methyl ketones (Goh et al., 2012). Analysis of the culture overlay of strain EHYL01 (Δ*pot1*) by GC/MS resulted in 62.6 mg/L total methyl ketones, demonstrating a 1,250-fold increase in methyl ketones compared to the parent strain PO1f. This finding supports the hypothesis that *Y. lipolytica* encodes at least one thioesterase that is capable of hydrolyzing β-ketoacyl-CoAs.

3.2. Detection of saturated, mono- and diunsaturated methyl ketones in the C_{13}-C_{23} range

Deletion of *pot1* resulted in accumulation of a broad range of saturated and unsaturated methyl ketones with different chain lengths (Fig. 2). Mainly odd-chain saturated methyl ketones ranging from 2-tridecanone (C13:0) to 2-tricosanone (C23:0), with 2-heptadecanone (C17:0) as the

predominant species, were detected. Surprisingly, even-chain saturated methyl ketones in the range from 2-tetradecanone (C14:0) to 2-docosanone (C22:0) were also identified. For compound verification, the observed mass spectra were matched to the mass spectra of the corresponding putative methyl ketones listed in the database of the National Institute of Standards and Technology (NIST) (Linstrom and Mallard, 2001). Even though no NIST mass spectra were available for 2-eicosanone (C20:0), 2-heneicosanone (C21:0), and 2-tricosanone (C23:0) (Fig. S1-S3), several factors indicate that the observed mass spectra belong to the putative compounds: (i) their mass spectral fragmentation pattern is highly similar to the ones of the annotated long-chain methyl ketones, (ii) their chromatographic retention time increases in a logical magnitude of a CH_2-group, and (iii) the molecular ion peaks of *m/z* 296, *m/z* 310 and *m/z* 338, respectively, correspond to their relative molecular mass.

In addition to saturated methyl ketones, monounsaturated 2-pentadecenone (C15:1) and 2-heptadecenone (C17:1) were detected. The mass spectrum of 2-pentadecenone was reported previously (Goh et al., 2012). 2-heptadecenone shows a highly similar mass spectral fragmentation pattern (Fig. S4). Its molecular ion peak of *m/z* 252 corresponds to the relative molecular mass of 2-heptadecanone lacking two protons resulting from the formation of one double bond. It can be concluded that the C17:1 peak is (*Z*)-8-heptadecen-2-one derived from oleic acid (18:1 fatty acid), the most abundant fatty acid in the PO1f base strain (Blazeck et al., 2014). Furthermore, in the total ion chromatogram small amounts of diunsaturated 2-trididecenone (C13:2), 2-pentadidecenone (C15:2), and 2-heptadidecenone (C17:2) were observed (Fig. S5-S7).

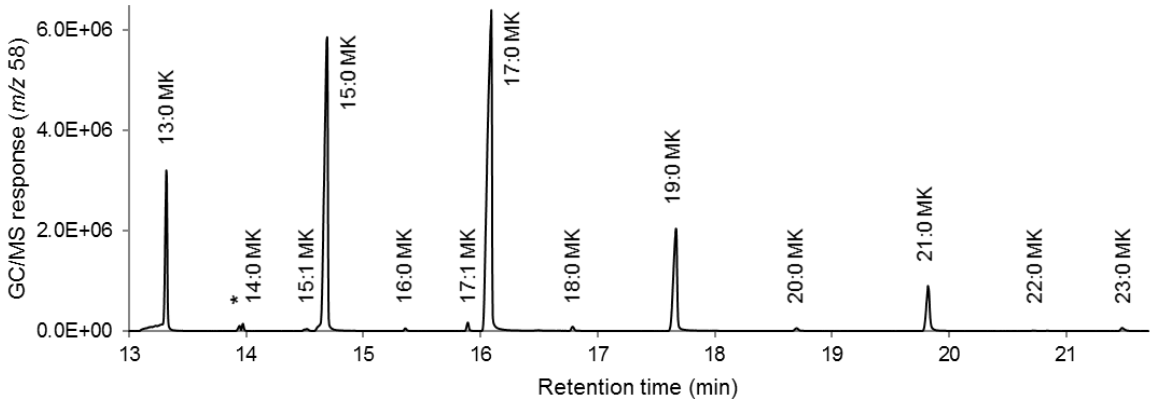

Fig. 2. Methyl ketone production in strain EHYL01 (Δ*pot1*). The GC extracted-ion chromatogram (*m/z* 58) of the dodecane overlay from a culture of strain EHYL01 (Δ*pot1*). Methyl ketones were assigned to their according peaks. The carbon chain length X and the degree of unsaturation Y are indicated for each X:Y methyl ketone (MK). *, internal standard 3-tetradecanone.

3.3. Peroxisomal targeting of heterologous methyl ketone pathway enzymes improves production

To increase the metabolic flux towards methyl ketone biosynthesis, we integrated a bacterial heterologous pathway developed by Goh and co-workers (Goh et al., 2012). It consists of the acyl-CoA oxidase ACO from *Micrococcus luteus* (*Mlut*_11700), the multifunctional enzyme FadB (*Ec*DH1_4135), and the thioesterase FadM (*Ec*DH1_3166), both from *E. coli* (Fig. 1). *Yarrowia lipolytica* contains six acyl-CoA oxidases, encoded by genes *POX1* to *POX6*, exhibiting different substrate specificities and activity levels (Fickers et al., 2005; Wang et al., 1999a; Wang et al., 1999b). The global acyl-CoA oxidase enzyme is imported as a heteropentameric complex into the peroxisome (Titorenko et al., 2002). *M. luteus* ACO, on the other hand, is encoded by a single gene and was reported to be highly soluble (Goh et al., 2012). By overexpressing ACO and FadB, we anticipated an increase in the intracellular pool of β-ketoacyl-CoAs, which can subsequently be hydrolyzed to β-keto acids by FadM.

In contrast to prokaryotes where fatty acids are broken down in the cytoplasm, in yeast and other eukaryotic cells, β-oxidation of long-chain fatty acids occurs exclusively in peroxisomes. Incorporating the bacterial pathway would require targeting the involved heterologous enzymes to

the peroxisomal matrix. In fact, engineering the cell to produce methyl ketones in peroxisomes, in lieu of the cytoplasm as it has been done in *E. coli* and *R. eutropha* (Goh et al., 2012; Müller et al., 2013), may reduce the detrimental effect of reactive oxygen species (ROS) that arise from peroxidation and lipid oxidation. Hydrogen peroxide is formed during the FAD-dependent oxidation of acyl-CoA to *trans*-2,3-dehydroacyl-CoA by both the native and the heterologous acyl-CoA oxidase (Fig. 1). Furthermore, lipid peroxides are generated by oxidation of unsaturated fatty acids and facilitate the formation of highly reactive electrophilic aldehydes (Li et al., 2011; Xu et al., 2017). These molecules impair cell viability by promoting cell aging and disabling enzymes (Grimsrud et al., 2008; Xu et al., 2017; Zimniak, 2011). However, compartmentalization of the methyl ketone biosynthesis pathway would shield the cell from elevated oxidative stress, which may be caused by pulling the metabolic flux towards β-oxidation and facilitate detoxification of hydrogen peroxide by naturally occurring peroxidases.

Targeting heterologous enzymes to peroxisomes typically requires a peroxisome targeting signal (PTS) to be added to their peptide sequence. The C-terminal tripeptide Ala-Lys-Leu (AKL) has been identified to be crucial for import of the *Y. lipolytica* MFE into peroxisomes and has been considered a consensus PTS for *Y. lipolytica* (Madzak, 2015; Smith et al., 2000). It was employed to target a bacterial polyhydroxyalkanoate (PHA) synthase to the peroxisomal matrix for PHA production (Haddouche et al., 2010). We decided to employ an alternative PTS for peroxisomal import of the heterologous methyl ketone pathway enzymes – the C-terminal tripeptide Ser-Lys-Leu (SKL) – which has previously been demonstrated to efficiently localize green fluorescent protein (GFP) and RedStar2 fluorescent protein to the peroxisome in *Y. lipolytica* (Dulermo et al., 2015; Xue et al., 2013).

Since the first three reactions of β-oxidation can be catalyzed by the native *Y. lipolytica* enzymes POX1-POX6 and MFE (Fig. 1), providing a peroxisomal pool of β-ketoacyl-CoAs, we chose FadM to be the first heterologous enzyme to be introduced to pull the metabolic flux towards production of β-keto acids. The effect of peroxisomal targeting was tested by individually

overexpressing two different versions of FadM. The *fadM* coding sequences were cloned into the vector pMCS-UAS1B$_{16}$-TEF-Cre (Blazeck et al., 2013). The first version contains the unaltered codon-optimized *fadM*, the translational product of which localizes to the cytoplasm. The second version harbors the codon-optimized *fadM* and nine additional nucleotides encoding the SKL tripeptide immediately preceding the stop codon. Plasmids were transformed into the Δ*pot1* strain EHYL01 and analyzed for methyl ketone production. The strain overexpressing FadM-SKL demonstrated a 6.5-fold increase in methyl ketone accumulation compared to the parent strain EHYL01 harboring the control plasmid pSL16-CEN1-1(227) in minimal medium (Fig. 3A). Surprisingly, overexpression of FadM lacking the PTS reduced methyl ketone biosynthesis 10-fold. This finding suggests that adding the tripeptide SKL targets FadM for import into the peroxisomal matrix and that inefficient localization would result in a significant decrease in methyl ketone titers. Subsequently, *fadM*-SKL was integrated into the genome of EHYL01 (Δ*pot1*) by homologous recombination yielding strain EHYL10 (Δ*pot1*, *fadM*-SKL). Heterologous methyl ketone pathway genes were integrated into the genome to allow for iterative strain development and reuse of the marker. Furthermore, it allows to cultivate strains in non-selective media. Growing EHYL10 in YPD rich medium improved methyl ketone production 1.8-fold compared to EHYL01 (Fig. 3B).

After integrating *fadM*-SKL into strain EHYL01, we sought to push the metabolic flux towards biosynthesis of β-keto acids by increasing the pool of available β-ketoacyl-CoAs. This was achieved by overexpressing and targeting ACO and FadB to the peroxisome using the same PTS that had been employed to import FadM into the peroxisomal matrix (Fig. 1). The genes *aco*-SKL and *fadB*-SKL were integrated into the genome of strain EHYL10 as a single DNA construct yielding strain EHYL12 (Δ*pot1*, *fadM*-SKL, *fadB*-SKL, *aco*-SKL). Unlike *fadM*-SKL, which was cloned downstream of a constitutive hybrid promoter (Blazeck et al., 2014), *fadB*-SKL and *aco*-SKL are driven by strong native constitutive promoters containing expression-enhancing introns (Damude et al., 2011; Tai and Stephanopoulos, 2013). Integration of these two genes into strain EHYL10 (Δ*pot1*, *fadM*-SKL) further increased the methyl ketone titer by 1.34-fold in YPD rich medium. The ultimate strain, EHYL12 (Δ*pot1*, *fadM*-SKL,

fadB-SKL, *aco*-SKL), accumulated methyl ketones to a titer of 151.5 mg/L (± 4.2 mg/L), which represents a 3,000-fold improvement compared to the *Y. lipolytica* base strain PO1f (Fig. 3B).

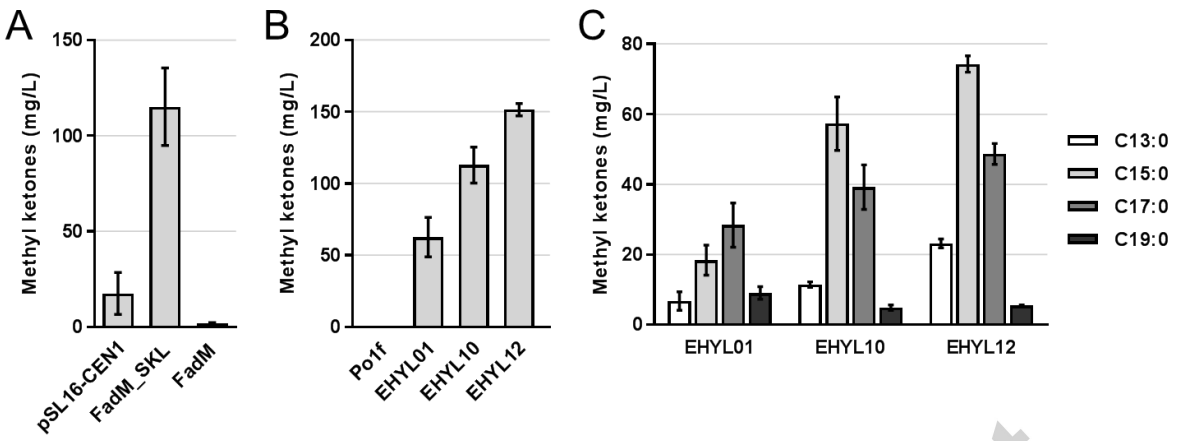

Fig. 3. Methyl ketone titers of strains with an engineered β-oxidation pathway. (A) Methyl ketone accumulation of strain EHYL01 (Δ*pot1*) overexpressing FadM-SKL or FadM in selective minimal medium from an episomal vector. pSL16-CEN1-1(227) was employed as a control plasmid. (B) Total methyl ketone titers of strains EHYL01 (Δ*pot1*), EHYL10 (Δ*pot1*, *fadM*-SKL), and EHYL12 (Δ*pot1*, *fadM*-SKL, *fadB*-SKL, *aco*-SKL) cultivated in YPD rich medium. (C) The concentrations of the individual saturated methyl ketone species 2-tridecanone, 2-pentadecanone, 2-heptadecanone, and 2-nonadecanone in the three engineered strains. Error bars represent standard deviations of at least three biological replicates.

3.4. Methyl ketone composition in strains with an engineered β-oxidation pathway

The methyl ketone composition of the best producing strain EHYL12 (Δ*pot1*, *fadM*-SKL, *fadB*-SKL, *aco*-SKL) comprises: 2-tridecanone (15%), 2-pentadecanone (49%), 2-heptadecanone (32%), and 2-nonadecanone (4%) (Fig. 3C). For quantification of total methyl ketones produced in culture tubes, only the four most abundant saturated species were taken into account.

A shift in methyl ketone composition was observed when *fadM*-SKL was integrated into EHYL01 (Δ*pot1*) (Fig. 3C). Two-heptadecanone is the predominant methyl ketone produced by EHYL01. In strains EHYL10 and EHYL12, however, which both express FadM-SKL, 2-pentadecanone is the most abundantly produced species. Noticeably, the titers of methyl ketones with chain lengths of

less than or equal to 17 carbons were highest in EHYL12 and lowest in EHYL01, whereas the titers of methyl ketones with a chain length of more than 18 carbons were lowest in EHYL12 and highest in EHYL01. This may reflect the chain length preference of the *E. coli* thioesterase FadM for acyl-CoA substrates between C_{12} and C_{18} (Nie et al., 2008). Alternatively, this could result from simply increasing flux towards methyl ketones.

The shift in methyl ketone composition from mainly 2-heptadecanone (C17:0) in EHYL01 towards predominantly 2-pentadecanone (C15:0) in EHYL10 and EHYL12 is beneficial for the mixture of methyl ketones to be applied as biofuel blending agent. Most important, the melting point of a compound is lowered with decreasing chain length.

3.5. Influence of oxygen on biosynthesis of methyl ketones

Attempts to scale up cultures of strain EHYL01 (Δ*pot1*) to assess methyl ketone production in larger volumes resulted in the discovery that the dissolved oxygen (DO) level in a culture substantially influences methyl ketone biosynthesis. Initially, the dependence on available oxygen was evaluated for 50-mL cultures of EHYL01 in baffled and non-baffled shake flasks. Baffles generate additional turbulence increasing the overall oxygen transfer rate and therefore enhancing the DO level. GC/MS analysis of the dodecane overlays demonstrated that in baffled shake flasks, methyl ketone production was completely abolished. This is in contrast to the methyl ketone accumulation of cultures grown in non-baffled shake flasks, which was similar to the 10-mL cultures cultivated in tubes.

The reduction in methyl ketone titers was hypothesized to be caused by an increase in ROS due to over-oxygenation of the culture. Elevated levels of ROS have been reported to negatively impact the accumulation of fatty acids as well as to lead to a transition in cell morphology (Xu et al., 2017). Xu and co-workers engineered a *Y. lipolytica* strain to harbor several oxidative stress defense mechanisms. When exposed to higher levels of ROS, this strain exhibited round and singular cell morphology, whereas the non-engineered strain developed pseudohyphal and mycelial structures (Xu et al., 2017). To illustrate the influence of over-oxygenation on lipid formation and cell

morphology in the *pot1*-deficient strain EHYL01, we evaluated cultures grown in non-baffled and baffled shake flasks by microscopy after staining the cells with Nile red. Nile red is commonly used for visualization of lipid bodies (Greenspan et al., 1985). It was observed that the different conditions do not seem to have an effect on lipid abundance and distribution (Fig. 4). However, cells grown in baffled shake flasks (Fig. 4A) appeared to develop larger vacuoles compared to a culture in non-baffled shake flasks (Fig. 4B).

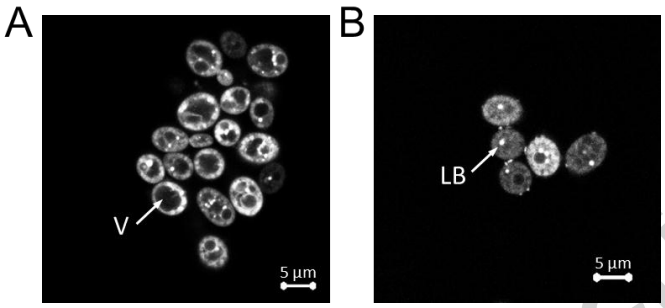

Fig. 4. Change of cell morphology caused by different levels of dissolved oxygen. *Y. lipolytica* EHYL01 was stained with Nile red after cultivation in (A) baffled shake flasks allowing higher dissolved oxygen concentrations and (B) non-baffled shake flasks. Vacuoles (V) and lipid bodies (LB) are indicated.

3.6. Bioreactor cultivation of the optimal producing strain

Bioreactor growth studies of the wild type strain PO1f and the optimal producing strain EHYL12 (Δ*pot1*, *fadM*-SKL, *fadB*-SKL, *aco*-SKL) were performed to monitor production of methyl ketones in fully controlled bioreactors. Cultivations were carried out in 0.5-L vessels containing 0.3 L of YPD medium. Different levels of DO and control parameters were initially tested before settling on the final cultivation conditions. No methyl ketones were detected at 40% DO, supporting our findings from the shake flask experiments. The highest methyl ketone levels were obtained at 5% DO. Another optimization iteration was required to maintain the desired yeast cell morphology, since transition from single cells to hyphal growth was observed when the control cascade was set as a function of agitation speed. Only when agitation was maintained constant over the cultivation and the inlet air was chosen as the variable in the DO cascade, the strain EHYL12 remained as single cell over the course of the cultivation.

Consumption of glucose, cellular growth, production of methyl ketones, and other metabolites including succinate, pyruvate, acetate, and mannitol were monitored for both strains. Compared to the wild type strain (Fig. 5A), EHYL12 demonstrates no difference in terms of cellular growth and consumption of glucose (0.22 g/L/h) (Fig. 5B). However, while the parent strain does not demonstrate accumulation of methyl ketones, their production in the engineered strain clearly correlates with glucose consumption (Fig. S8). After its depletion, a second feed of glucose was pulsed into the bioreactors with strain EHYL12 to further boost methyl ketone biosynthesis. The final titer of 314.8 mg/L with a process yield of 0.0073 g/g glucose represents more than a 6,000-fold titer improvement over parental strain grown in culture tubes. For calculation of the final titer, unsaturated methyl ketones were also taken into account (Fig. 5C). However, as for the test tube cultures of strain EHYL12, primarily saturated methyl ketones contribute to the overall titer. Interestingly, three additional species of methyl ketones could be identified to accumulate in the bioreactor cultivations (Fig. S9). C15:1a corresponds to (*Z*)-8-2-pentadecen-2-one, which has already been detected in the test tube cultures. C13:1a was not observed in the test tube cultures, however, its mass spectral fragmentation pattern has been reported previously (Goh et al., 2012). The fragmentation patterns of C13:1b and C15:1b (Fig. S10 and S11) differ from the reported mass spectra of C13:1a and C15:1a. This suggests a variation in the location of the double bond.

Succinate and pyruvate were the main by-products for both strains. Whereas no significant difference ($p < 0.05$) was observed in the case of pyruvate (1.02 g/L and 0.92 g/L in strains PO1f and EHYL12, respectively), a significant reduction ($p < 0.05$) of succinate levels was observed at the end of the first batch phase in strain EHYL12 (2.05 g/L) compared to the wild type strain PO1f (2.47 g/L) (Fig. 6). Up to 1.80 g/L pyruvate and 4.86 g/L succinate were accumulated at the end of the cultivation of strain EHYL12. Acetate levels were found to remain constant at a low level, whereas mannitol titers increased throughout the cultivation (Fig. S12). Mannitol accumulation was demonstrated to decrease the levels of ROS and therefore, is an indicator for oxidative stress in *Y. lipolytica* (Xu et al., 2017). However, the mannitol concentration of 8 mM at the end of cultivation is much lower than

the previously reported titers (Xu et al., 2017), suggesting that reducing the level of DO also minimizes oxidative stress.

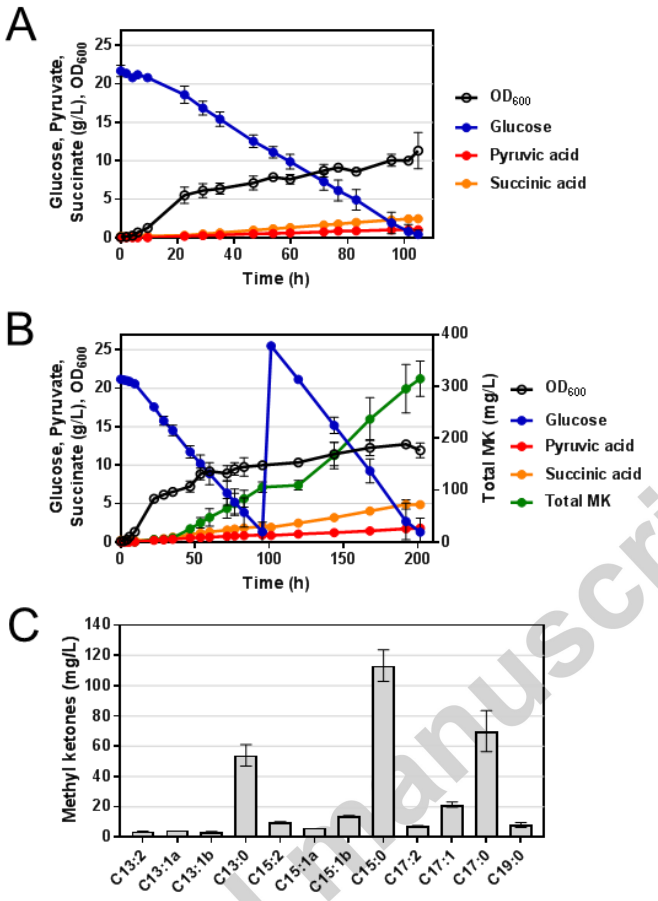

Fig. 5. Performance of the wild type strain PO1f (A) and the engineered strain EHYL12 (B) in bioreactor cultivations. (C) Distribution of methyl ketones produced by strain EHYL12 at the final time point. The chain length X and the degree of unsaturation Y is indicated for each X:Y methyl ketone. Error bars represent standard deviations of three biological replicates.

3.7 Conversion of cytosolic acyl-CoAs into free fatty acids promotes methyl ketone biosynthesis

An understanding of fatty acid transport and activation mechanisms is essential when the product of interest, such as methyl ketones, is interlinked with β-oxidation. In the cytosol, free fatty acids (FFA) are either bound by the fatty acid binding protein, activated by the acyl-CoA synthetase FAA1, or transported into the peroxisome for β-oxidation via an ANT1-dependent pathway. Activated fatty acids are also able to enter the peroxisome via the heterodimer PXA1/PXA2, or stored as TAGs in

lipid bodies (Dulermo et al., 2015). In contrast to *S. cerevisiae*, in *Y. lipolytica* activation of fatty acids targeted for β-oxidation occurs mainly in peroxisomes rather than in the cytosol (Dulermo et al., 2015).

The linear relationship between glucose consumption and methyl ketone production in strain EHYL12 (Fig. 5B, Fig. S8) suggests that under our growth conditions cytosolic FFAs rapidly enter peroxisomes to a greater degree than being directed toward the storage pathway. Therefore, it is worth investigating whether an increase in accessible FFAs, which can ultimately be targeted for β-oxidation, results in improved methyl ketone biosynthesis. This was tested by overexpressing a number of acyl-CoA thioesterases that catalyze the conversion of acyl-CoAs into FFAs. Overexpression and cytosolic targeting of several thioesterases have previously been shown to increase FFA secretion in a strain being unable to produce lipid bodies, activate, or degrade FFAs (Δ*faa1* Δ*mfe* Q4) (Ledesma-Amaro et al., 2016). To assess the effect of localization, we overexpressed one cytosolic enzyme (YALI0E18876p; TEc1), two mitochondrial enzymes (YALI0C15230p; TEm2 and YALI0C22121p; TEm3), one peroxisomal enzyme (YALI0F14729p), and one thioesterase lacking a known targeting signal (YALI0D03597p) (Table 2). The thioesterase genes were individually cloned into the overexpression vector pMCS-UAS1B$_{16}$-TEF-Cre (Blazeck et al., 2013) and separately transformed into the POT1-deficient strain EHYL01.

GC/MS analysis of the dodecane overlay revealed that overexpression of TEc1 in strain EHYL01 resulted in a four-fold increase in methyl ketone titers as compared to EHYL01 transformed with the control plasmid pSL16-CEN1-1(227) (Yamane et al., 2008) (Fig. 6A). Individual overexpression of the other thioesterases did not contribute to a statistically significant ($p < 0.05$) increase in methyl ketone accumulation. To evaluate the contribution of TEc1 to overall methyl ketone biosynthesis, the chromosomal *TEc1* was deleted in EHYL01 (Δ*pot1*), yielding EHYL08 (Δ*pot1*, Δ*TEc1*). The *TEc1*-deficient strain showed a two-fold decrease in methyl ketone titer compared to EHYL01 (Fig. 6B). It is noteworthy that the compositions of methyl ketones in EHYL01, EHYL08, and the TEc1 overexpressing strain (EHYL01 pEH047) are similar. Additionally no growth defects were

observed when TEc1 was overexpressed in EHYL01, suggesting that the toxicity associated with FFA accumulation (Dulermo et al., 2015) is efficiently bypassed.

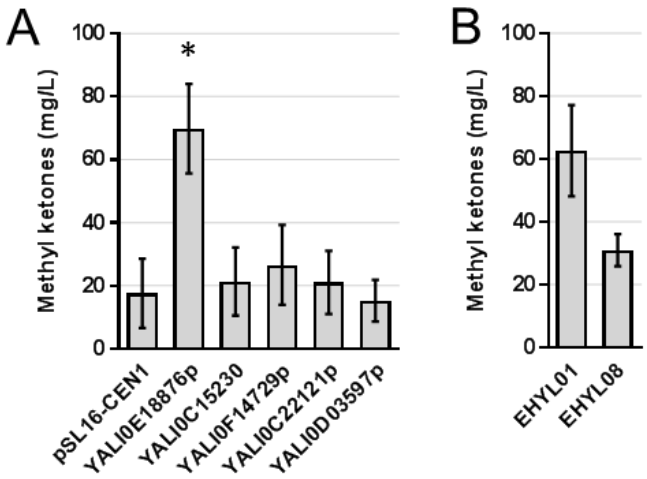

Fig. 6. The influence of endogenous acyl-CoA thioesterases on methyl ketone production in strain EHYL01. (A) Methyl ketone accumulation of strain EHYL01 overexpressing different endogenous acyl-CoA thioesterases in selective minimal medium from an episomal vector. pSL16-CEN1-1(227) was employed as a control plasmid. Thioesterases are indicated by their protein identifier. (B) Methyl ketone production of strain EHYL01 (Δ*pot1*) and EHYL08 (Δ*pot1*, Δ*TEc1*) cultivated in YPD rich medium. Error bars represent standard deviations of at least four biological replicates. Asterisks indicate statistically significant differences in methyl ketone titers when compared to pSL16-CEN1-1(227) for $p < 0.05$ (unpaired *t* test).

4. Discussion

Fatty acid-derived biofuels from non-edible lignocellulosic feedstocks are sustainable alternatives to petroleum-based fuel. They emit less greenhouse gases and air pollutants, are compatible with current transportation infrastructure, and their production does not require land with high agricultural value (Hill et al., 2006). *Y. lipolytica* is an attractive microbial chassis for the industrial production of fatty acid-derived compounds. Here, we engineered *Y. lipolytica* β-oxidation to produce long- and very long-chain methyl ketones.

Chromosomal deletion of the gene encoding the peroxisomal acetyl-CoA acyltransferase, POT1, led to a 1,250-fold increase in methyl ketone accumulation when compared to the parent strain PO1f. 2-Heptadecanone (C17:0) was found to be the prominent methyl ketone in strain EHYL01 (Δ*pot1*). In addition to odd-chain methyl ketones, which derive from even-chain fatty acids, small amounts of even-chain methyl ketones were detected which ultimately derive from odd-chain fatty acids. Blazeck and co-workers hypothesized the synthesis of less-favored odd-chain fatty acids to result from a highly active lipogenesis (Blazeck et al., 2014). The chain lengths of the observed methyl ketones correlate with the fatty acid profile reported for *Y. lipolytica* PO1f (Blazeck et al., 2014). The degree of unsaturation, however, is altered in the methyl ketone accumulating strain. Oleic acid (C18:1) is the most abundant fatty acid with eighteen carbons followed by stearic acid (C18:0) and linoleic acid (C18:2) in PO1f (Blazeck et al., 2014), whereas the resulting monounsaturated methyl ketone (C17:1) in strain EHYL01 only slightly contributes to the final methyl ketone titer. The observed divergence may be due to a higher availability of saturated free fatty acids. Monounsaturated acyl-CoAs are the preferred substrates for acylation reactions and are therefore the predominant species in membranes and lipid bodies (Qiao et al., 2015).

Successful peroxisomal localization of heterologous bacterial methyl ketone pathway enzymes was found to be crucial for product formation. In selective minimal medium, episomal overexpression of FadM-SKL increased methyl ketone accumulation 6.5-fold, whereas overexpression of FadM, lacking a PTS, decreased methyl ketone synthesis 10-fold compared to EHYL01 (Δ*pot1*). The

adverse effect of a cytosolic localized FadM may be explained by its promiscuous activity toward several acyl-CoA thioesters (Nie et al., 2008). These thioesters might be hydrolyzed into dead-end, free acid products (Goh et al., 2014). However, the strain expressing the cytosolic FadM did neither demonstrate an increased secretion of fatty acids, nor did it show growth defects which have been associated with high intracellular levels of FFAs (Dulermo et al., 2015). This might suggest that these fatty acids are either bound by sterol carrier proteins or transported into the mitochondria to escape toxicity (Dulermo et al., 2015; Ferreyra et al., 2006). The metabolic flux towards β-ketoacyl-CoAs was increased by integrating the genes *fadB*-SKL and *aco*-SKL. This is the first report of the bacterial methyl ketone biosynthesis pathway developed by Goh and co-workers (Goh et al., 2012) to be targeted to a cellular organelle and applied in a eukaryotic organism. Whereas *E. coli* and *R. eutropha* mainly produced medium-chain methyl ketones, a broad range of very long-chain methyl ketones up to 2-tricosanone (C23:0) were detected in *Y. lipolytica*, and these products may serve other commercial applications.

Optimization of DO concentration was found to impact methyl ketone biosynthesis. In β-oxidation, oxygen is utilized in the first reaction for the reduction of FAD (Fig. 1). Furthermore, it is required for the subsequent oxidation of $FADH_2$ and $NADH+H^+$ to prevent redox imbalance. Consequently, high levels of oxygen would be expected to improve the catabolism of fatty acids. However, shake flask experiments and batch bioreactor cultivations of the methyl ketone producing strains EHYL01 and EHYL12, respectively, demonstrated that the highest tested level of oxygenation resulted in reduced methyl ketone biosynthesis. The decrease in product titers may be explained by elevated levels of ROS generated in oxygen-rich environments. In particular, unsaturated fatty acids such as oleic acid (C18:1) or linoleic acid (C18:2) are highly susceptible to hydroxyl radical-induced oxidation (Xu et al., 2017). This correlates with our observation that vacuoles had increased in size when cells had been grown under oxygen-replete conditions (Fig. 4). Vacuoles play an important role in the cellular oxidative stress response (Nishikawa et al., 2016). Therefore, the presence of larger vacuoles may be a consequence of enhanced ROS detoxification activity. On the other hand,

insufficiently low levels of DO trigger the morphological transition from single cells to hyphal growth and methyl ketone production was also inhibited. As reported by Bellou and co-workers, DO levels should be considered the major factor affecting *Y. lipolytica* morphology (Bellou et al., 2014), and therefore any oxygen-dependent product. In conclusion, the oxygen level is a key parameter for methyl ketone biosynthesis, and optimizing titer will require balanced aeration to protect the cells from oxidative stress, to prevent mycelia formation, but also to guarantee an efficient regeneration of cofactors during β-oxidation.

The cytosolic acyl-CoA thioesterase TEc1 supplied most of the FFAs that were targeted for β-oxidation in EHYL01. This is in accordance with previously reported data where overexpression of TEc1 resulted in the highest intracellular FFA titer amongst several thioesterases tested (Ledesma-Amaro et al., 2016). A similar concentration of FFAs was achieved overexpressing TEm2 in the cytosol. In our study, however, the mitochondrial targeting signal was not removed. Its mitochondrial localization might explain why overexpression of TEm2 did not translate into a similar methyl ketone titer as it was achieved using TEc1. Furthermore, it can be concluded that TEc1 has no preference for acyl-CoA chain length since the methyl ketone compositions produced by EHYL01 (Δ*pot1*), the TEc1 overexpressing strain (EHYL01 pEHYl047), and the *TEc1*-deficient strain, EHYL08 (Δ*pot1*, Δ*TEc1*) are the same.

This study is the first attempt to produce acyl-thioester-derived methyl ketones in *Y. lipolytica*. Engineering methyl ketone biosynthesis in this yeast species is of particular importance in light of its robust performance in industrial fermentation and its history of use in commercial processes. Methyl ketone production was shown to linearly correlate with glucose consumption. We speculate that future engineering strategies directed towards uncoupling acetyl-CoA production from nitrogen starvation, overproduction and targeting cytosolic fatty acids to peroxisomes will allow for continuous biosynthesis of methyl ketones during controlled fed-batch fermentation to improve product titer and yield. Alternative pathways for the supply of cytosolic acetyl-CoA have successfully been implemented in *Y. lipolytica* and it was demonstrated that lipid biosynthesis could be

uncoupled from nitrogen starvation (Xu et al., 2016). Furthermore, engineering approaches that have previously been pursued to prevent lipid degradation may be reversed to facilitate methyl ketone biosynthesis. For example, deletion of *pex10*, encoding a protein essential for peroxisome biogenesis and proliferation, resulted in a significant increase in lipid accumulation due to dysfunctional peroxisomes (Xue et al., 2013). Overexpression of PEX10 in turn may result in more active peroxisomal β-oxidation.

The methyl ketones synthesized by EHYL12 are mainly saturated, unbranched, and of long chain-length. These structural features benefit biofuel properties such as cetane number, exhaust emission, or oxidative stability, whereas their melting points are less favorable (Knothe and Dunn, 2003). The overall melting point could be lowered by increasing the proportion of monounsaturated methyl ketones, which may be realized by improving mobilization and activation of unsaturated fatty acids. Another approach would be to alter the chain length of fatty acids by introducing acyl-ACP or acyl-CoA thioesterases. Hybrid thioesterases, being composed of the fungal fatty acid synthase and a bacterial thioesterase, have been reported to significantly increase the portions of C_{12} and C_{14} fatty acids in *Y. lipolytica* (Xu et al., 2016). In combination with desaturation, the resulting methyl ketones would exhibit excellent biofuel properties (Goh et al., 2012).

5. Conclusion

In this study, we engineered the oleaginous yeast *Y. lipolytica* to produce long- and very long-chain methyl ketones ranging from C_{13}-C_{23}. The constructed strain comprises a truncated peroxisomal β-oxidation to facilitate the accumulation of β-ketoacyl-CoAs, and an integrated heterologous pathway composed of FadB, ACO and FadM. These enzymes were incorporated to improve the natural flux towards β-ketoacyl-CoAs and catalyze their hydrolysis to β-keto acids. Peroxisomal targeting of FadB, ACO and FadM was found to be crucial for efficient methyl ketone production. Furthermore, it was demonstrated that the level of available oxygen is an important factor that should be taken into account when engineering cellular β-oxidation. In our case, it had a significant effect on cell morphology and product formation. Overall, this work highlights the potential of peroxisomes to be employed as compartments for heterologous metabolic pathways. They give yeast a considerable advantage over bacteria such as *E. coli* or *R. eutropha* which lack these organelles. Bioreactor fermentations of our best producing strain resulted in 314.8 mg/L methyl ketones. We believe that *Y. lipolytica* will serve as a superior host for high-titer biosynthesis of methyl ketones. This research will serve as a foundation for future efforts towards commercial production of long-chain methyl ketones from non-food lignocellulosic feedstocks.

Acknowledgements

This work was part of the DOE Joint BioEnergy Institute (http://www.jbei.org) supported by the U. S. Department of Energy, Office of Science, Office of Biological and Environmental Research, through contract DE-AC02-05CH11231 between Lawrence Berkeley National Laboratory and the U. S. Department of Energy. This work was also supported by the National Science Foundation grant MCB 1330914. VSN, KJR, CAS, and GTB thank the Co-Optimization of Fuels & Engines (Co-Optima) project sponsored by the U. S. Department of Energy (DOE) Office of Energy Efficiency and Renewable Energy (EERE), Bioenergy Technologies and Vehicle Technologies Offices. We would like to thank Hal Alper and Leo d'Espaux for providing plasmids and strains, Ee-Been Goh and Harry R. Beller for useful discussions, and all members of JBEI who helped to carry out this research. CMD, EKH, VSN, and KJR designed the experiments. EKH, CMD, VSN, WL, KJR, and CAS performed the experiments. EKH, CMD, VSN, KJR, GTB, and JDK analyzed the data and wrote the manuscript. All authors read and approved the final manuscript.

Conflict of interest

JDK has financial interests in Amyris, Lygos, Demetrix, Constructive Biology, Maple Bio and Napigen.

Table 1. Strains used and generated in this study.

Strain	Genotype	Reference or source
E. coli strains		
HST08	F- *ara* Δ*(lac-proAB) [4Φ80d lacZΔM15] rpsL(str) thi* Δ*(mrr-hsdRMS-mcrBC)* Δ*mcrA dam dcm*	Clontech Laboratories Inc.
Y. lipolytica strains		
PO1f	*matA, leu2-270, ura3-302, xpr2-322, axp1-2*	(Madzak et al., 2000)
EHYL01	PO1f, Δ*pot1*	This study
EHYL08	EHYL01, Δ*TEc1*	This study
EHYL10	EHYL01, UAS1B$_1$-TEF-*fadM*-SKL	This study
EHYL12	EHYL10, GPDin-*fadB*-SKL, FBAin-*aco*-SKL	This study

Table 2. *Y. lipolytica* acyl-CoA thioesterase genes that were analyzed for their influence on methyl ketone biosynthesis.

Gene identifier	Uniprot ID	Name	Localization	Reference
YALI0E18876g	Q6C5D9	TEc1	Cytosol	(Dulermo et al., 2015)
YALI0C15230g	B5FVC4	TEm2	Mitochondria	(Dulermo et al., 2015)
YALI0F14729g	Q6C1N6	N/A	Peroxisome	This study
YALI0C22121g	Q6CB40	TEm3	Mitochondria	(Dulermo et al., 2015)
YALI0D03597g	Q6CAE2	N/A	N/A	This study

References

Angerbauer, C., Siebenhofer, M., Mittelbach, M., Guebitz, G., 2008. Conversion of sewage sludge into lipids by *Lipomyces starkeyi* for biodiesel production. Bioresour. Technol. 99**,** 3051-3056. https://doi.org/10.1016/j.biortech.2007.06.045.

Barth, G., Gaillardin, C., 1997. Physiology and genetics of the dimorphic fungus *Yarrowia lipolytica*. FEMS Microbiol. Rev. 19**,** 219-237. https://doi.org/10.1111/j.1574-6976.1997.tb00299.x.

Batth, T. S., Keasling, J. D., Petzold, C. J., 2012. Targeted proteomics for metabolic pathway optimization. In: Keller NP, Turner G, editors. Fungal Secondary Metabolism: Methods and Protocols. Humana Press. p. 237-249. https://doi.org/10.1007/978-1-62703-122-6_17.

Bellou, S., Makri, A., Triantaphyllidou, I.-E., Papanikolaou, S., Aggelis, G., 2014. Morphological and metabolic shifts of *Yarrowia lipolytica* induced by alteration of the dissolved oxygen concentration in the growth environment. Microbiology. 160**,** 807-817. https://doi.org/10.1099/mic.0.074302-0.

Beopoulos, A., Cescut, J., Haddouche, R., Uribelarrea, J.-L., Molina-Jouve, C., Nicaud, J.-M., 2009. *Yarrowia lipolytica* as a model for bio-oil production. Prog. Lipid Res. 48**,** 375-387. https://doi.org/10.1016/j.plipres.2009.08.005.

Blazeck, J., Hill, A., Liu, L., Knight, R., Miller, J., Pan, A., Otoupal, P., Alper, H. S., 2014. Harnessing *Yarrowia lipolytica* lipogenesis to create a platform for lipid and biofuel production. Nat. Commun. 5**,** 3131. https://doi.org/10.1038/ncomms4131.

Blazeck, J., Liu, L., Knight, R., Alper, H. S., 2013. Heterologous production of pentane in the oleaginous yeast *Yarrowia lipolytica*. J. Biotechnol. 165**,** 184-194. https://doi.org/10.1016/j.jbiotec.2013.04.003.

Bourel, G., Nicaud, J.-M., Nthangeni, B., Santiago-Gomez, P., Belin, J.-M., Husson, F., 2004. Fatty acid hydroperoxide lyase of green bell pepper: cloning in *Yarrowia lipolytica* and biogenesis of volatile aldehydes. Enzyme Microb. Technol. 35**,** 293-299. https://doi.org/10.1016/j.enzmictec.2003.12.014.

Chen, D.-C., Beckerich, J.-M., Gaillardin, C., 1997. One-step transformation of the dimorphic yeast *Yarrowia lipolytica*. Appl. Microbiol. Biotechnol. 48**,** 232-235. https://doi.org/10.1007/s002530051043.

Chi, Z., Zheng, Y., Jiang, A., Chen, S., 2011. Lipid production by culturing oleaginous yeast and algae with food waste and municipal wastewater in an integrated process. Appl. Biochem. Biotechnol. 165**,** 442-453. https://doi.org/10.1007/s12010-011-9263-6.

Clomburg, J. M., Blankschien, M. D., Vick, J. E., Chou, A., Kim, S., Gonzalez, R., 2015. Integrated engineering of β-oxidation reversal and ω-oxidation pathways for the synthesis of medium chain ω-functionalized carboxylic acids. Metab. Eng. 28**,** 202-212. https://doi.org/10.1016/j.ymben.2015.01.007.

d'Espaux, L., Mendez-Perez, D., Li, R., Keasling, J. D., 2015. Synthetic biology for microbial production of lipid-based biofuels. Curr. Opin. Chem. Biol. 29**,** 58-65. https://doi.org/10.1016/j.cbpa.2015.09.009.

Damude, H. G., Gillies, P. J., Macool, D. J., Picataggio, S. K., Pollak, D. M. W., Ragghianti, J. J., Xue, Z., Yadav, N. S., Zhang, H., Zhu, Q. Q., High eicosapentaenoic acid producing strains of *Yarrowia lipolytica*. Google Patents, 2011.

Dulermo, R., Gamboa-Meléndez, H., Ledesma-Amaro, R., Thévenieau, F., Nicaud, J.-M., 2015. Unraveling fatty acid transport and activation mechanisms in *Yarrowia lipolytica*. Biochim. Biophys. Acta, Mol. Cell. Biol. Lipids. 1851**,** 1202-1217. https://doi.org/10.1016/j.bbalip.2015.04.004.

Feng, X., Lian, J., Zhao, H., 2015. Metabolic engineering of *Saccharomyces cerevisiae* to improve 1-hexadecanol production. Metab. Eng. 27**,** 10-19. https://doi.org/10.1016/j.ymben.2014.10.001.

Ferreyra, R. G., Burgardt, N. I., Milikowski, D., Melen, G., Kornblihtt, A. R., Dell'Angelica, E. C., Santomé, J. A., Ermácora, M. R., 2006. A yeast sterol carrier protein with fatty-acid and fatty-

acyl-CoA binding activity. Arch. Biochem. Biophys. 453, 197-206. https://doi.org/10.1016/j.abb.2006.06.024.

Fickers, P., Benetti, P.-H., Wache, Y., Marty, A., Mauersberger, S., Smit, M., Nicaud, J.-M., 2005. Hydrophobic substrate utilisation by the yeast *Yarrowia lipolytica*, and its potential applications. FEMS Yeast Res. 5, 527-543. https://doi.org/10.1016/j.femsyr.2004.09.004.

Fickers, P., Le Dall, M., Gaillardin, C., Thonart, P., Nicaud, J., 2003. New disruption cassettes for rapid gene disruption and marker rescue in the yeast *Yarrowia lipolytica*. J. Microbiol. Methods. 55, 727-737. https://doi.org/10.1016/j.mimet.2003.07.003.

Forney, F., Markovetz, A., 1971. The biology of methyl ketones. J. Lipid Res. 12, 383-395.

Galafassi, S., Cucchetti, D., Pizza, F., Franzosi, G., Bianchi, D., Compagno, C., 2012. Lipid production for second generation biodiesel by the oleaginous yeast *Rhodotorula graminis*. Bioresour. Technol. 111, 398-403. https://doi.org/10.1016/j.biortech.2012.02.004.

Gao, S., Tong, Y., Zhu, L., Ge, M., Zhang, Y., Chen, D., Jiang, Y., Yang, S., 2017. Iterative integration of multiple-copy pathway genes in *Yarrowia lipolytica* for heterologous β-carotene production. Metab. Eng. 41, 192-201. https://doi.org/10.1016/j.ymben.2017.04.004.

Gibson, D. G., Young, L., Chuang, R.-Y., Venter, J. C., Hutchison, C. A., Smith, H. O., 2009. Enzymatic assembly of DNA molecules up to several hundred kilobases. Nat. Methods. 6, 343-345. https://doi.org/10.1038/nmeth.1318.

Goh, E.-B., Baidoo, E. E., Burd, H., Lee, T. S., Keasling, J. D., Beller, H. R., 2014. Substantial improvements in methyl ketone production in *E. coli* and insights on the pathway from in vitro studies. Metab. Eng. 26, 67-76. https://doi.org/10.1016/j.ymben.2014.09.003.

Goh, E.-B., Baidoo, E. E., Keasling, J. D., Beller, H. R., 2012. Engineering of bacterial methyl ketone synthesis for biofuels. Appl. Environ. Microbiol. 78, 70-80. https://doi.org/10.1128/AEM.06785-11.

Greenspan, P., Mayer, E. P., Fowler, S. D., 1985. Nile red: a selective fluorescent stain for intracellular lipid droplets. J. Cell Biol. 100, 965-973. https://doi.org/10.1083/jcb.100.3.965.

Grimsrud, P. A., Xie, H., Griffin, T. J., Bernlohr, D. A., 2008. Oxidative stress and covalent modification of protein with bioactive aldehydes. J. Biol. Chem. 283, 21837-21841. https://doi.org/10.1074/jbc.R700019200.

Haddouche, R., Delessert, S., Sabirova, J., Neuvéglise, C., Poirier, Y., Nicaud, J.-M., 2010. Roles of multiple acyl-CoA oxidases in the routing of carbon flow towards β-oxidation and polyhydroxyalkanoate biosynthesis in *Yarrowia lipolytica*. FEMS Yeast Res. 10, 917-927. https://doi.org/10.1111/j.1567-1364.2010.00670.x.

Hill, J., Nelson, E., Tilman, D., Polasky, S., Tiffany, D., 2006. Environmental, economic, and energetic costs and benefits of biodiesel and ethanol biofuels. Proc. Natl. Acad. Sci. U.S.A. 103, 11206-11210. https://doi.org/10.1073/pnas.0604600103.

Hillson, N. J., Rosengarten, R. D., Keasling, J. D., 2011. j5 DNA assembly design automation software. ACS Synth. Biol. 1, 14-21. https://doi.org/10.1021/sb2000116.

Knothe, G., Dunn, R. O., 2003. Dependence of oil stability index of fatty compounds on their structure and concentration and presence of metals. J. Am. Oil Chem. Soc. 80, 1021-1026. https://doi.org/10.1007/s11746-003-0814-x.

Ledesma-Amaro, R., Dulermo, R., Niehus, X., Nicaud, J.-M., 2016. Combining metabolic engineering and process optimization to improve production and secretion of fatty acids. Metab. Eng. 38, 38-46. https://doi.org/10.1016/j.ymben.2016.06.004.

Lee, M. E., DeLoache, W. C., Cervantes, B., Dueber, J. E., 2015. A highly characterized yeast toolkit for modular, multipart assembly. ACS Synth. Biol. 4, 975-986. https://doi.org/10.1021/sb500366v.

Li, Q., Bai, Z., O'Donnell, A., Harvey, L., Hoskisson, P., McNeil, B., 2011. Oxidative stress in fungal fermentation processes: the roles of alternative respiration. Biotechnol. Lett. 33, 457-467. https://doi.org/10.1007/s10529-010-0471-x.

Li, Q., Du, W., Liu, D., 2008. Perspectives of microbial oils for biodiesel production. Appl. Microbiol. Biotechnol. 80, 749-756.

Linstrom, P. J., Mallard, W., 2001. NIST Chemistry webbook; NIST standard reference database No. 69.

Liu, H., Bi, X., Huo, M., Lee, C.-f. F., Yao, M., 2012. Soot emissions of various oxygenated biofuels in conventional diesel combustion and low-temperature combustion conditions. Energy & Fuels. 26**,** 1900-1911. https://doi.org/10.1021/ef201720d.

Longo, M. A., Sanromán, M. A., 2006. Production of food aroma compounds: microbial and enzymatic methodologies. Food Technol. Biotechnol. 44**,** 335-353.

Madzak, C., 2015. *Yarrowia lipolytica*: recent achievements in heterologous protein expression and pathway engineering. Appl. Microbiol. Biotechnol. 99**,** 4559-4577. https://doi.org/10.1007/s00253-015-6624-z.

Madzak, C., Tréton, B., Blanchin-Roland, S., 2000. Strong hybrid promoters and integrative expression/secretion vectors for quasi-constitutive expression of heterologous proteins in the yeast *Yarrowia lipolytica*. J. Mol. Microbiol. Biotechnol. 2**,** 207-216.

Mason, R. T., Fales, H. M., Jones, T. H., Pannell, L. K., Chinn, J. W., Crews, D., 1989. Sex pheromones in snakes. Science. 245**,** 290-293.

Müller, J., MacEachran, D., Burd, H., Sathitsuksanoh, N., Bi, C., Yeh, Y.-C., Lee, T. S., Hillson, N. J., Chhabra, S. R., Singer, S. W., 2013. Engineering of *Ralstonia eutropha* H16 for autotrophic and heterotrophic production of methyl ketones. Appl. Environ. Microbiol. 79**,** 4433-4439. https://doi.org/10.1128/AEM.00973-13.

Nie, L., Ren, Y., Schulz, H., 2008. Identification and characterization of *Escherichia coli* thioesterase III that functions in fatty acid β-oxidation. Biochemistry. 47**,** 7744-7751. https://doi.org/10.1021/bi800595f.

Nishikawa, H., Miyazaki, T., Nakayama, H., Minematsu, A., Yamauchi, S., Yamashita, K., Takazono, T., Shimamura, S., Nakamura, S., Izumikawa, K., 2016. Roles of vacuolar H+-ATPase in the oxidative stress response of *Candida glabrata*. FEMS Yeast Res. 16**,** fow054. https://doi.org/10.1093/femsyr/fow054.

Park, J., Rodríguez-Moyá, M., Li, M., Pichersky, E., San, K.-Y., Gonzalez, R., 2012. Synthesis of methyl ketones by metabolically engineered *Escherichia coli*. J. Ind. Microbiol. Biotechnol. 39**,** 1703-1712. https://doi.org/10.1007/s10295-012-1178-x.

Patel, A., Arora, N., Sartaj, K., Pruthi, V., Pruthi, P. A., 2016. Sustainable biodiesel production from oleaginous yeasts utilizing hydrolysates of various non-edible lignocellulosic biomasses. Renewable Sustainable Energy Rev. 62**,** 836-855. https://doi.org/10.1016/j.rser.2016.05.014.

Peralta-Yahya, P. P., Keasling, J. D., 2010. Advanced biofuel production in microbes. Biotechnol. J. 5**,** 147-162. https://doi.org/10.1002/biot.200900220.

Pfleger, B. F., Gossing, M., Nielsen, J., 2015. Metabolic engineering strategies for microbial synthesis of oleochemicals. Metab. Eng. 29**,** 1-11. https://doi.org/10.1016/j.ymben.2015.01.009.

Pignède, G., Wang, H., Fudalej, F., Gaillardin, C., Seman, M., Nicaud, J.-M., 2000. Characterization of an extracellular lipase encoded by LIP2 in *Yarrowia lipolytica*. J. Bacteriol. 182**,** 2802-2810. https://doi.org/10.1128/JB.182.10.2802-2810.2000.

Qiao, K., Abidi, S. H. I., Liu, H., Zhang, H., Chakraborty, S., Watson, N., Ajikumar, P. K., Stephanopoulos, G., 2015. Engineering lipid overproduction in the oleaginous yeast *Yarrowia lipolytica*. Metab. Eng. 29**,** 56-65. https://doi.org/10.1016/j.ymben.2015.02.005.

Qiao, K., Wasylenko, T. M., Zhou, K., Xu, P., Stephanopoulos, G., 2017. Lipid production in *Yarrowia lipolytica* is maximized by engineering cytosolic redox metabolism. Nat. Biotechnol. 35**,** 173-177. https://doi.org/10.1038/nbt.3763.

Ratledge, C., Wynn, J. P., 2002. The biochemistry and molecular biology of lipid accumulation in oleaginous microorganisms. In: Laskin AI, Bennett JW, Gadd GM, editors. Advances in Applied Microbiology. Academic Press.

Schrader, J., Etschmann, M., Sell, D., Hilmer, J.-M., Rabenhorst, J., 2004. Applied biocatalysis for the synthesis of natural flavour compounds–current industrial processes and future prospects. Biotechnol. Lett. 26**,** 463-472. https://doi.org/10.1023/B:BILE.0000019576.80594.0e.

Sheehan, J., Camobreco, V., Duffield, J., Graboski, M., Shapouri, H., Life cycle inventory of biodiesel and petroleum diesel for use in an urban bus. National Renewable Energy Lab, Golden, CO, 1998. https://doi.org/10.2172/658310.

Smith, J. J., Brown, T. W., Eitzen, G. A., Rachubinski, R. A., 2000. Regulation of peroxisome size and number by fatty acid β-oxidation in the yeast *Yarrowia lipolytica*. J. Biol. Chem. 275**,** 20168-20178. https://doi.org/10.1074/jbc.M909285199.

Stärkle, M., Die Methylketone im oxydativen Abbau einiger Triglyceride (bzw. Fettsäuren) durch Schimmelpilze unter Berücksichtigung der besonderen Ranzidität des Kokosfettes. 1924. https://doi.org/10.3929/ethz-a-000122285.

Tai, M., Stephanopoulos, G., 2013. Engineering the push and pull of lipid biosynthesis in oleaginous yeast *Yarrowia lipolytica* for biofuel production. Metab. Eng. 15**,** 1-9. https://doi.org/10.1016/j.ymben.2012.08.007.

Thoms, H., 1903. Über die Wertbestimmung des Nelkenöles. Arch. Pharm. 241**,** 592-603. https://doi.org/10.1007/978-3-642-51331-2_14.

Titorenko, V. I., Nicaud, J.-M., Wang, H., Chan, H., Rachubinski, R. A., 2002. Acyl-CoA oxidase is imported as a heteropentameric, cofactor-containing complex into peroxisomes of *Yarrowia lipolytica*. J. Cell Biol. 156**,** 481-494. https://doi.org/10.1083/jcb.200111075.

Walbaum, H., Hüthig, O., 1902. Ueber das Ceylon-Zimmtöl. J. Prakt. Chem. 66**,** 47-58. https://doi.org/10.1002/prac.19020660104.

Wang, H., Le Dall, M.-T., Waché, Y., Laroche, C., Belin, J.-M., Nicaud, J.-M., 1999a. Cloning, sequencing, and characterization of five genes coding for Acyl-CoA oxidase isozymes in the yeast *Yarrowia lipolytica*. Cell Biochem. Biophys. 31**,** 165-174. https://doi.org/10.1007/BF02738170.

Wang, H. J., Le Dall, M.-T., Waché, Y., Laroche, C., Belin, J.-M., Gaillardin, C., Nicaud, J.-M., 1999b. Evaluation of acyl coenzyme A oxidase (Aox) isozyme function in the n-alkane-assimilating yeast *Yarrowia lipolytica*. J. Bacteriol. 181**,** 5140-5148.

Williams, C. G., 1858. On the constitution of the essential oil of rue. Philos. Trans. R. Soc. London. 148**,** 199-204. http://www.jstor.org/stable/108658.

Xu, P., Qiao, K., Ahn, W. S., Stephanopoulos, G., 2016. Engineering *Yarrowia lipolytica* as a platform for synthesis of drop-in transportation fuels and oleochemicals. Proc. Natl. Acad. Sci. U.S.A. 113**,** 10848-10853. https://doi.org/10.1073/pnas.1607295113.

Xu, P., Qiao, K., Stephanopoulos, G., 2017. Engineering oxidative stress defense pathways to build a robust lipid production platform in *Yarrowia lipolytica*. Biotechnol. Bioeng. 114**,** 1521-1530. https://doi.org/10.1002/bit.26285.

Xue, Z., Sharpe, P. L., Hong, S.-P., Yadav, N. S., Xie, D., Short, D. R., Damude, H. G., Rupert, R. A., Seip, J. E., Wang, J., 2013. Production of omega-3 eicosapentaenoic acid by metabolic engineering of *Yarrowia lipolytica*. Nat. Biotechnol. 31**,** 734-740. https://doi.org/10.1038/nbt.2622.

Yamane, T., Sakai, H., Nagahama, K., Ogawa, T., Matsuoka, M., 2008. Dissection of centromeric DNA from yeast *Yarrowia lipolytica* and identification of protein-binding site required for plasmid transmission. J. Biosci. Bioeng. 105**,** 571-578. https://doi.org/10.1263/jbb.105.571.

Yu, X., Zheng, Y., Dorgan, K. M., Chen, S., 2011. Oil production by oleaginous yeasts using the hydrolysate from pretreatment of wheat straw with dilute sulfuric acid. Bioresour. Technol. 102**,** 6134-6140. https://doi.org/10.1016/j.biortech.2011.02.081.

Zimniak, P., 2011. Relationship of electrophilic stress to aging. Free Radical Biol. Med. 51**,** 1087-1105. https://doi.org/10.1016/j.freeradbiomed.2011.05.039.

Highlights

- Engineered *Y. lipolytica* β-oxidation to produce long- and very long-chain methyl ketones in the C_{13}-C_{23} range.
- Targeted a heterologous bacterial methyl ketone biosynthesis pathway to the peroxisome.
- Level of dissolved oxygen has been found to substantially impact the biosynthesis of methyl ketones.
- Best strain produced 314.8 mg/L of methyl ketones from glucose in bioreactor cultivations, representing more than a 6,000-fold improvement over the parental strain.